Helicity in Ropes of Chiral Nanotubes: Calculations and Observation

David Teich, Gotthard Seifert, Sumio Iijima, and David Tománek

Phys. Rev. Lett. **108**, 235501 — Published 4 June 2012

DOI: 10.1103/PhysRevLett.108.235501

Helicity in ropes of chiral nanotubes: calculations and observation

David Teich,[1] Gotthard Seifert,[1] Sumio Iijima,[2] and David Tománek[3,*]

[1] *Physikalische Chemie, Technische Universität Dresden, D-01062 Dresden, Germany*
[2] *Faculty of Science and Technology, Meijo University, Nagoya, Aichi 468-8502, Japan*
[3] *Physics and Astronomy Department, Michigan State University, East Lansing, Michigan 48824-2320, USA*

Even though isolated defect-free single-wall carbon nanotubes (SWCNTs) are straight, bundles of chiral SWCNTs are often helical according to our observations using high-resolution electron microscopy. The driving force for the formation of such helices is the energy gain associated with the optimum orientational alignment of neighboring nanotubes. Our total energy calculations allow to analyze the torsional and bending stress components in helical nanotube ropes and specify, under which conditions straight nanotube bundles gain energy upon forming a helix.

PACS numbers: 61.48.De, 62.25.-g 61.46.-w

Helical coiling or helicity occurs quite often in natural structures, with proteins and DNA being prominent examples, and has attracted early interest of Physicists[1]. The general cause underlying the formation of helices is steric hindrance. To a certain degree, hindrance may also be caused by the anisotropy in the interaction of aligned tubes or wires, including single-wall carbon nanotubes (SWCNTs)[2]. It is well known that SWCNTs form stable, close-packed bundles[3]. Yet little attention has been paid so far to whether free-standing bundles of defect-free SWCNTs are straight or helical. Presence of torsion, in turn, is known to open or modify the band gap at the Fermi level of SWCNTs[4–6] and thus to affect significantly the conductance of nanotube ropes. Also, helical coiling may stabilize nanotube ropes structurally and thus improve their mechanical properties over non-coiled nanotube arrays.

Here we show high-resolution electron micrographs of helical structures in free-standing SWCNT ropes. Although isolated nanotubes are straight, bundles of chiral SWCNTs may benefit energetically from coiling to a helix. We find that such helices form when the energy gain associated with optimum orientational alignment of coiled adjacent nanotubes outweighs the coiling stress. Our total energy calculations allow us to analyze the torsional and bending stress components in helical nanotube ropes and to specify, under which conditions coiling of straight nanotube bundles is energetically favorable.

Our total energy calculations for isolated and bundled carbon nanotubes have been performed using a simplified density functional theory based method with a local orbital basis[7]. This method has been successfully applied to a variety of carbon structures[7] and subsequently extended to accommodate van der Waals interactions[8], including their proper description in graphitic systems[8]. We use its adaptation for systems with helical symmetry[9], which is essential for the efficient treatment of chiral nanotubes [10–12] and helical ropes.

The SWCNTs observed in this study have been synthesized using the laser ablation method. In this technique, carbon is vaporized inside a 3 cm diameter quartz tube by exposing a target graphite rod containing Fe catalyst to a pulsed YAG laser beam. Evaporated carbon and the laser plasma gas are initially ejected from the target surface opposite to the carrier gas flow direction, followed by condensation to SWCNTs in the cool helium carrier gas during the next few seconds and are free of defects to a high degree[13, 14]. Next, the SWCNTs and the plasma gas are pushed back by the carrier gas and follow the gas flow direction. We have noticed that the nanotubes are subject to a severe gas turbulence during this turnover process, which allows them to explore their configurational freedom including twisting, bending and interaction with other nanotubes to find an optimum configuration in a rope. Eventually, nanotube ropes aggregate to form spider-web like structures, in which the individual SWCNTs are kinetically frozen due to their high aspect ratio. For the reasons given above, we believe that the structure of SWCNT ropes prepared using laser ablation should provide valuable information about the equilibrium geometry.

We performed extensive observations of the nanotube structure in SWCNT samples using a high-resolution transmission electron microscope (Topcon 002B, operated at 200 keV) with a point-to-point resolution of $\lesssim$2 Å. Our observations revealed a common occurrence of helical coiling in SWCNT ropes. A typical and also simple example of such helical coiling is presented in Fig. 1(a), which shows a pair of coiled SWCNTs prepared using the laser ablation method. Both tubes have nearly the same diameter of 14 Å and the helix displays a pitch length $\lambda = 1220$ Å. Another typical image, presented in Fig. 1(b), is a close-packed rope of seven SWCNTs with a hexagonal cross-section and a pitch length $\lambda \approx 1600$ Å. Similar helical coiling has also been observed in bundles of few multi-wall nanotubes with rope radii ranging from $50 - 200$ nm[15].

To understand the reason for helical coiling in bundles of nanotubes, we compared the energy components associated with helical coiling of isolated nanotubes to the inter-tube interaction, which depends on the relative

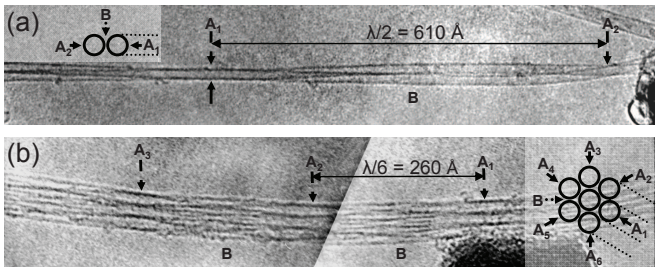

FIG. 1. High-resolution transmission electron micrograph of a free-standing rope containing (a) two and (b) seven SWCNTs. The local rope orientation changes along the helix with respect to the electron beam direction, indicated by parallel dotted lines in the insets. Only two dark lines corresponding to the projections of SWCNT walls along the incident electron beams should occur in a two-tube rope for orientations labeled A_1 and A_2 in (a), shown also in Fig. 2(a), separated by half the pitch length. Only four such lines are observed in the 7-tube rope in (b) for rope orientations $A_1 - A_6$, separated by $\lambda/6$.

orientation of the tubes along the helix. These energy components can be best discussed using the schematic representation of helices and ropes in Fig. 2. Similar to two graphene layers, which favor energetically a specific stacking structure and require an activation energy for displacement[8, 16], also two parallel achiral nanotubes favor energetically specific orientations and require an activation energy for rotation[2], shown in Fig. 3(a). Adjacent straight chiral nanotubes, on the other hand, do not benefit in the optimum way from the anisotropy in the inter-tube interaction.

Deforming a nanotube of radius R to a helix (coil) of pitch length λ and radius ρ, defined in Fig. 2(b), corresponds to local bending and torsion and requires the energy

$$E_{coil} = E_{bend} + E_{tors}\,. \tag{1}$$

In the case of small local curvatures, corresponding to large helical radii or pitch lengths, the bending energy per length segment s of the nanotube can be written as

$$E_{bend}/s = \frac{1}{2} k_{bend} \kappa^2\,, \tag{2}$$

where the local curvature κ is

$$\kappa = \frac{1}{\rho\,(1+\mu^2)} \tag{3}$$

and the slope μ is given by

$$\mu = \frac{\lambda}{2\pi\rho}\,. \tag{4}$$

Forming a coil is associated not only with bending, but also with torsion. In the linear regime, the torsion energy per nanotube length segment s is given by

$$E_{tors}/s = \frac{1}{2} k_{tors} \tau^2\,, \tag{5}$$

with the torsion τ related to the helix radius and slope by

$$\tau = \frac{\mu}{\rho\,(1+\mu^2)}\,. \tag{6}$$

In the special case of a coil with zero radius ρ, the bending energy component of E_{coil} vanishes and the torsion energy becomes $E_{tors} = (1/2)k_{tors}(\varphi/s)^2$, where φ/s is the change in the orientation φ per length s.

Similar to graphite, the inter-tube interaction E_i consists of van der Waals and weak covalent interactions[14], caused by a small overlap of carbon $p_\perp$ orbitals on adjacent tubes[16]. As shown in Fig. 3(a), the maximum rotational barrier for two (10,10) nanotubes amounts to $\lesssim$0.5 meV/atom. These barriers are the basis for representing nanotubes as helical gears in Figs. 2(c-d) and 3(a).

Numerical values for the bending and torsional force constants were obtained by subjecting nanotubes with specific chiral indices (n, m) to bending and torsion. Since the resistance of a graphene monolayer to stretching, bending and shear is nearly isotropic, also k_{bend} and k_{tors} depend primarily on the nanotube radius R. This is shown in Fig. 3(b); in particular the R^3 dependence of the bending force constant agrees with predictions from elasticity theory[17].

The energy associated with deforming a $(10, 10)$ nanotube to a helix of changing radius, while keeping the slope μ constant, is shown in Fig. 3(c) along with the schematic view of the helix for two different radii ρ_1 and ρ_2. Especially for large values of ρ, the agreement between the numerical results and the analytical expression is very good. Only at helix radii below the $(10, 10)$ nanotube radius $R = 6.8$ Å we observe a serious deviation from the analytical results due to the strong deformation of the nanotube[18]. This regime is not of interest for

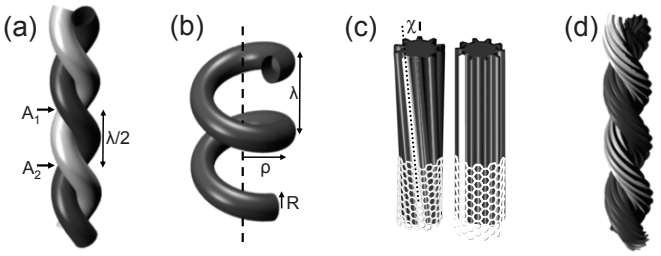

FIG. 2. Structure of carbon nanotubes and their bundles. (a) A pair of coiled nanotubes as the simplest example of a helical rope. Schematic views of (b) an individual nanotube helix, (c) chiral and achiral nanotubes, with emphasis on the pitch angle χ associated with the direction of lines of hexagons along the tube, shown by the white solid line, and (d) the optimum entanglement of two chiral nanotubes. The labels in (a) refer to Fig. 1(a). The pitch length λ and the radius ρ of an individual helix, formed of a nanotube of radius R, are shown in (b).

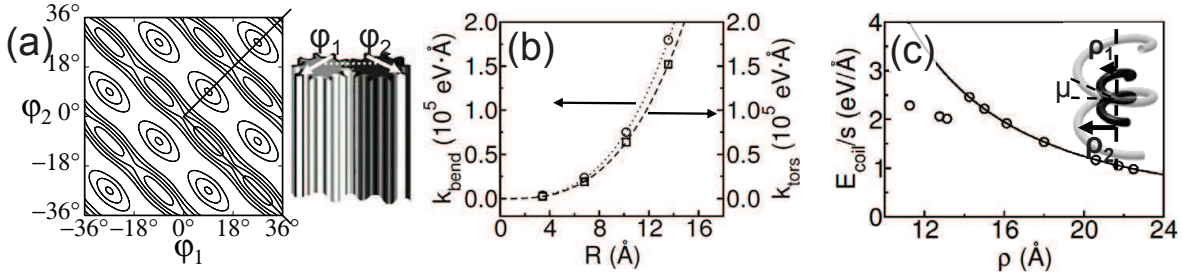

FIG. 3. Energies associated with the formation of helical nanotube bundles. (a) Results of Ref. 2 for the interaction energy profile per atom between two parallel (10,10) carbon nanotubes at equilibrium distance. The equipotential lines are separated by 0.1 meV/atom and the tube orientations φ_1 and φ_2 are defined in the schematic sketch. (b) Bending (◯) and torsional (□) force constants as a function of the nanotube radius R. (c) Coiling energy in helices of constant slope μ as a function of ρ. The data points for a $(10,10)$ nanotube in (c) are compared to analytical data based on Eq. (1).

this study, since the helix radius in a rope is larger than the optimum value $\rho_e = R + d_i/2$, where $d_i = 3.14$ Å is the equilibrium inter-wall distance.

Having established the validity range of our model, we proceed to provide general criteria for the formation of helical nanotube ropes. In the following we focus on nanotubes of the same handedness with $n > m$, since they represent well the entire range of competing interactions. Nanotubes of different handedness, in particular matching pairs of (n,m) and (m,n) nanotubes, are less interesting, since the chiral structures compensate and do not cause helical coiling.

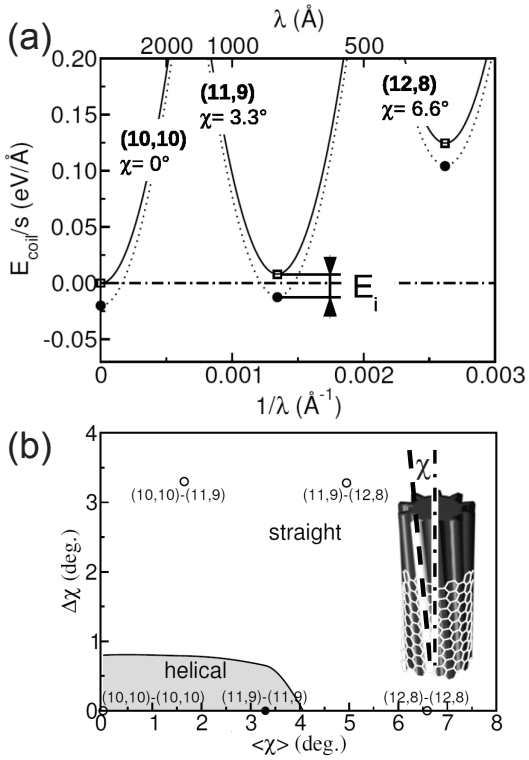

FIG. 4. Energy considerations for the formation of helical ropes. (a) Coiling energy E_{coil} per nanotube length s of two identical nanotubes in the case of ideal orientational alignment along the helix, shown by the solid lines. Presence of the inter-tube interaction E_i stabilizes the helix, as indicated by the dotted lines. The energy reference is a pair of non-interacting (10,10) nanotubes. (b) Schematic phase diagram, indicating conditions, under which two nanotubes with pitch angles χ_1 and χ_2 should form a helix. $<\chi>=(\chi_1+\chi_2)/2$ is the average pitch angle and $\Delta\chi = |\chi_1 + \chi_2|$ is the pitch angle difference.

To see whether the anisotropic inter-tube interaction E_i may stabilize helical coiling in a rope containing two identical nanotubes, we first twisted each individual nanotube so that the pitch angle χ, shown in Fig. 2(c), would become zero. Then, the two nanotubes were attached to each other along the imaginary white lines, emphasized in Fig. 2(c), and allowed to release the torsional stress by forming a helix. We plot the corresponding coiling energy E_{coil}, obtained using Eq. (1), as a function of the pitch length λ in Fig. 4(a) for a pair of achiral $(10,10)$ and chiral $(11,9)$ and $(12,8)$ nanotubes. Clearly, there is an optimum pitch length for each pair of nanotubes, indicated by the open squares in Fig. 4(a). Trivially, for a pair of axially aligned achiral $(10,10)$ nanotubes with the pitch angle $\chi = 0°$, no helical coiling is necessary to optimize the orientational alignment, and thus $\lambda \to \infty$. This is no longer true for ropes of chiral nanotubes, which require helical coiling with a finite pitch length to maintain orientational alignment.

As can be inferred from the comparison of the coiling energy for different nanotube pairs in Fig. 4(a), all helical ropes, including those with the optimum pitch length, are less stable than a pair of straight nanotubes if the inter-tube interaction would not play a role. With the anisotropic inter-tube interaction E_i, which provides extra stabilization for orientationally aligned nanotubes, the net energy change $E_{coil} + E_i$ may become negative for selected nanotube pairs, which would make a helical rope more stable than an axially aligned pair of straight chiral tubes. This is particularly true for nanotubes with small pitch angles, where E_{coil} is particularly small, such as for a pair of $(11,9)$ nanotubes with $\chi = 3.3°$. An

increasing value of χ results in a tighter helix with a smaller pitch length and a larger coiling energy that can no longer be compensated by the optimum gain in the inter-tube interaction, as seen in Fig. 3(a). Our results can be compared to the TEM observation in Fig. 1(a) of a helix with a pitch length $\lambda \approx 1220$ Å. The helix is formed by two nanotubes with a diameter of ≈14 Å, which may correspond to a $(10,10)$, $(11,9)$, or a $(12,8)$ nanotube. For identical tubes, we find that only the $(11,9)-(11,9)$ tube pair should form a stable helical rope, with an optimum pitch length $\lambda = 735$ Å. This nanotube pair may well represent that in Fig. 1(a) in spite of the considerably larger observed than calculated pitch length. We need to remember that the theoretical $T = 0$ estimate assumes the optimum tube alignment, which in reality is reduced by entropy as nanotubes vibrate at finite temperatures. The resulting reduction of the inter-tube interaction, seen near point *"B"* in Fig. 1(a), then causes an increase of the effective pitch length above the optimum $T = 0$ value. The coiling energy of a pair of $(12,8)$ nanotubes with a larger pitch angle and optimum pitch length of $\lambda = 380$ Å is too high to form a stable helix. A pair of achiral $(10,10)$ nanotubes forms a stable straight rope.

Using our analytical expressions for the deformation energy and the inter-tube interaction E_i, we can estimate the coiling energy for any pair of nanotubes and compare it to the optimum inter-tube interaction in order to judge, which tube pairs should form stable helices. Characterizing a nanotube of radius R primarily by its pitch angle χ, we expect that the tendency of a pair to form a stable helix depends primarily on the average pitch angle and the pitch angle difference. Our results are summarized as a schematic phase diagram[19] in Fig. 4(b). We find that helical ropes are formed primarily by homochiral tubes with $\Delta\chi = 0$, such as the $(11,9)-(11,9)$ pair discussed in Fig. 4(a). The stability island of helices is thus extremely narrow in the $\Delta\chi$ direction, and its boundary depends only weakly on the tube radius. We expect that the helical coiling should generally increase (and the rope pitch length decrease) with increasing $< \chi >$ and $\Delta\chi$ values. The strain increase in such tube pairs can no longer be compensated by the "lock-in" barrier in the anisotropic inter-tube interaction. The corresponding rope is then more stable in the "straight" than the "helical" configuration, as seen in Fig. 4(b). We note that, trivially, achiral nanotubes with $\chi = 0$ form straight ropes. Also heterochiral nanotubes, such as $(10,10)-(11,9)$ or $(11,9)-(12,8)$ pairs, prefer to form straight rather than helical ropes.

The energetic reasons for the formation of a helix apply, naturally, also to ropes containing more than two nanotubes, including the 7-tube rope in Fig. 1(b). With the likelihood of many pitch angles in the nanotube rope, the probability of ideal inter-tube orientational alignment is very small and the observed pitch length should be quite high. Our considerations for helical coiling energies are general and may lead to quantitatively different structural arrangements in other types of nanotubes and nanowires, including multi-wall carbon[15] and BN nanotubes.

In conclusion, we studied energetic reasons for defect-free carbon nanotubes to bundle to helical ropes and support our results by high-resolution electron microscopy observations. We find that the driving force for helical coiling in ropes is the energy gain associated with the optimum orientational alignment of neighboring nanotubes. Our total energy calculations, adapted to the helical symmetry, allowed us to analyze the torsional and bending stress components in helical nanotube ropes. For a pair of nanotubes as the simplest example of a rope, we identified the conditions, under which two aligned nanotubes gain energy upon forming a helix.

We acknowledge valuable contributions to the computational approach by Dong-Bo Zhang and Traian Dumitrica. This work was funded by the National Science Foundation under NSF-NSEC grant 425826 and NSF-NIRT grant ECS-0506309. GS was partly supported by the European Centre for Emerging Materials and Processes Dresden (ECEMP, project number: 10 13857/2379). The first author's visit to MSU was partially funded by the DAAD. Computational resources for this project were provided by the ZIH Dresden.

* E-mail: tomanek@pa.msu.edu

[1] J. W. Miller Jr., Phys. Rev. **14**, 129 (1902).
[2] Y.-K. Kwon and D. Tomanek, Phys. Rev. Lett. **84**, 1483 (2000), *ibid.* **106**, 219901 (2011)(E).
[3] A. Thess, R. Lee, P. Nikolaev, H. Dai, P. Petit, J. Robert, C. Xu, Y. H. Lee, S. G. Kim, A. G. Rinzler, D. T. Colbert, G. E. Scuseria, D. Tomanek, J. E. Fischer, and R. E. Smalley, Science **273**, 483 (1996).
[4] C. L. Kane and E. J. Mele, Phys. Rev. Lett. **78**, 1932 (1997).
[5] S. W. D. Bailey, D. Tomanek, Y. K. Kwon, and C. J. Lambert, Europhys. Lett. **59**, 75 (2002).
[6] T. Cohen-Karni, L. Segev, O. Srur-Lavi, S. R. Cohen, and E. Joselevich, Nat. Nano **1**, 36 (2006).
[7] D. Porezag, T. Frauenheim, T. Köhler, G. Seifert, and R. Kaschner, Phys. Rev. B **51**, 12947 (1995).
[8] L. Zhechkov, T. Heine, S. Patchkovskii, G. Seifert, and H. A. Duarte, J. Chem. Theory and Computation **1**, 841 (2005).
[9] D.-B. Zhang and T. Dumitrica, Appl. Phys. Lett. **93**, 031919 (2008).
[10] D.-B. Zhang, R. D. James, and T. Dumitrică, Phys. Rev. B **80**, 115418 (2009).
[11] E. Ertekin and D. C. Chrzan, Phys. Rev. B **72**, 045425 (2005).
[12] J. Alford, B. Landis, and J. Mintmire, Int. J. Quantum Chem. **105**, 767 (2005), 45th Annual Sanibel Symposium, Sanibel Isl, FL, MAR 05-11, 2005.
[13] The estimated nanotube formation temperature of

1200°C is relatively high, resulting in a much smaller concentration of atomic and structural defects than in nanotubes produced using chemical vapor deposition or arc discharge. In fact, high-resolution transmission electron microscope studies have not revealed any such defects in our samples.

[14] Presence of defects in nanotubes should modify in particular the inter-tube interaction energy and consequently change the pitch lenght of a helical rope.

[15] C.-J. Su, D. W. Hwang, S.-H. Lin, B.-Y. Jin, and L.-P. Hwang, PhysChemComm **5**, 34 (2002).

[16] R. H. Telling and M. I. Heggie, Phil. Mag. Lett. **83**, 411 (2003).

[17] Z. C. Tu and Z. C. Ou-Yang, J. Comput. Theor. Nanosci. **5**, 422 (2008), *ibid.* **5**, 1192 (2008)(E).

[18] B. I. Yakobson, C. J. Brabec, and J. Bernholc, Phys. Rev. Lett. **76**, 2511 (1996).

[19] Our calculations do not provide a simple analytical expression to distinguish between regions of stable helical and straight ropes. The separation line in Fig. 4(b) represents an extrapolation based on our numerical results.